Biochimica et Biophysica Acta, 778 (1984) 559–569
Elsevier

BBA 72386

DIELECTRIC ANALYSIS OF MITOCHONDRIA ISOLATED FROM RAT LIVER

I. SWOLLEN MITOPLASTS AS SIMULATED BY A SINGLE-SHELL MODEL

KOJI ASAMI [a,*], AKIHIKO IRIMAJIRI [a,*], TETSUYA HANAI [b], NORIYUKI SHIRAISHI [c,**] and KOZO UTSUMI [c]

[a] *Department of Physiology and* [c] *Department of Medical Biology, Kochi Medical School, Nankoku, Kochi 781-51 and* [b] *Laboratory of Dielectrics, Institute for Chemical Research, Kyoto University, Uji, Kyoto-fu 611 (Japan)*

(Received June 20th, 1984)

Key words: Dielectric dispersion; Mitoplast; Intramitochondrial structure; Membrane capacity; Permittivity; Conductivity; Single-shell model

A re-evaluation of the dielectric studies on isolated mitochondria (Pauly, H., Packer, L. and Schwan, H.P. (1960) J. Biophys. Biochem. Cytol. 7, 589-601, and ibid. 7, 603-612) is presented. The suspensions of 'mitoplasts' prepared from rat liver mitochondria by a hyposmotic (10 mM KCl) treatment showed a dielectric dispersion with its characteristic frequency lying in the 1–100 MHz range. In the analysis of data special emphasis was put on the choice of the theoretical models to employ after scrutiny of their applicability to the suspensions tested. As such we adopted the theory of Hanai et al. (Hanai, T., Asami, K., and Koizumi, N. (1979) Bull. Inst. Chem. Res., Kyoto Univ. 57, 297–305) that was advanced to include concentrated suspensions of shelled spheres. Curve fittings based on that theory resulted in a better agreement with experiment than the fittings based on a conventional theory for dilute suspensions. Major findings from our analyses on the swollen mitoplasts are that: (i) the limiting membrane of the mitoplasts has a specific electrical capacity of 1 $\mu F/cm^2$, (ii) the ratio of permittivity (or dielectric constant) for the mitoplast interior and permittivity for the external medium is 0.6–0.7, and (iii) the conductivity ratio between the interior phase and the medium is approx. 0.6. Reasons for discrepancy between the results of Pauly et al. and ours are discussed.

Introduction

The importance of mitochondria as the intracellular 'power plants' in the aerobic metabolism is now well established [1]. This concept has been borne out mainly from the collaboration of innumerable biochemical and ultrastructural studies accumulated hitherto. To further elaborate the whole view of mitochondrial function and organization, an entirely different approach is desirable. For instance, the study of passive electrical properties as revealed by a non-destructive means is expected to add much to the basic knowledge of the physical or electrical design of a mitochondrion which is made up of two compartments demarcated by the outer and inner membranes.

As early as in 1960, Pauly et al. [2,3] performed work along this line of approach reporting that the mitochondrion is surrounded by a limiting membrane whose electrical capacitance (C_m) is similar in value to that of cell membrane. Specifically, however, the reported data on C_m of approx. 0.5 $\mu F/cm^2$ for swollen hepatic mitochondria and of approx. 1.3 $\mu F/cm^2$ for cardiac counterparts seem

* Correspondence should be addressed to K.A. or A.I.
** Present address: Department of Radiation Medicine, Okayama University Medical School, Okayama 700, Japan.

to require revision to a certain extent since the analysis by Pauly et al. [2,3] was based on the approximate equations derived from the original Pauly-Schwan theory [4] for the shelled spheres. The approximations made by them are valid only for the suspension of particles in which membrane thickness d is negligibly small compared to particulate radius R. Indeed, as we pointed out previously [5], the use of the approximate forms instead of the general equation may lead to an erroneous estimate in the analyzed parameters such as C_m, unless the ratio $d/R < 10^{-3}$. With the particles approx. 1 μm in diameter the ratio d/R is of the order of 10^{-2} and therefore the error may become 30–40% [5].

In the present paper we describe the dielectric dispersion analysis of swollen mitoplasts with special emphasis put on the proper choice of models. The model and its theoretical framework we employed here have been proven sound and useful in the light of studies made by Hanai and co-workers [6] on an inanimate version of shelled spheres, i.e. the synthetic microcapsules in suspension. The results obtained are expected to revise data on the passive electrical properties of mitochondrial membranes and matrix. An accompanying paper [7] deals with the analysis of intact mitochondria based on a double-shell model.

Materials and Methods

Preparation and conditioning of mitoplasts

The isolation of rat liver mitochondria was based essentially on the method of Hogeboom [8] as modified by Utsumi [9]. After homogenization of livers in a preparation medium containing 0.25 M sucrose, 0.1 mM EDTA and 5 mM Tris-HCl (pH 7.4), the intact mitochondria were isolated using a 0.25 M/0.34 M sucrose gradient centrifugation procedure performed below 4°C. The purified mitochondria were washed twice in the preparation medium free of EDTA and then exposed to a hyposmotic shock by incubation in 10 mM KCl plus 10 mM Tris-HCl buffer (pH 7.4) for 1 h at 4°C. The resulting mitoplasts, after pelleted by centrifugation for 10 min at $10000 \times g$, were resuspended in the respective test media (media A and B, noted below) followed by incubation for 1–2 h either at 4°C or at 25°C. Occasionally, several combinations of the conditioning steps were employed, as specified in Results. In all cases, the specimens were washed, and finally suspended, in fresh test media immediately before the dielectric measurements. The composition of the test media was as follows: medium A, 130 mM KCl, 15 mM sucrose and 10 mM Tris-HCl (pH 7.4) with an osmolarity of 280 ± 10 mosM; medium B, 65 mM KCl and 10 mM Tris-HCl (pH 7.4) supplemented with an appropriate amount of sucrose to make medium B isosmotic with medium A.

Protein was determined according to the Hartree modification [10] of Lowry's method with bovine serum albumin as standard.

Electron microscopy and morphometry

Mitochondrial suspensions were diluted approx. 30-fold with a fixative of 1.75% glutaraldehyde in 50 mM cacodylate buffer (pH 7.4) and fixed overnight at 4°C. After centrifugation at $10000 \times g$ for 10 min, the pellets were post-fixed in 1% OsO_4 in the same buffer for 3–4 h, dehydrated in ethanol and embedded in Spurr's resin [11]. The osmolarity of the fixatives was adjusted to 280 ± 10 mosM by addition of sucrose. Ultrathin sections stained with uranyl acetate and lead citrate were examined with a Hitachi H-300 microscope. Magnification was determined by means of a carbon grating replica.

By assuming a spherical morphology for the mitoplasts, their stereologically 'true' radius was estimated from the volume-to-surface ratio (S_v) that was determined by the point counting method using Weibel's coherent multipurpose test systems [12]. In the present specimens, the effect of section thickness on S_v as assessed according to Weibel et al. [13] was found to be negligible owing to the section thickness well within 100 nm.

Dielectric measurements

Equivalent parallel capacitances (C) and conductances (G) for the mitoplast suspensions were measured, over a frequency range 0.1–500 MHz, by a computer-controlled analyzer system. The system consisted of Yokogawa-Hewlett-Packard RF- and LF-impedance analyzers (models 4191A and 4192A, respectively) coupled with a Hewlett-Packard 9825S desktop computer and a 7225A plotter via a GP-IB line. Data collection from 112

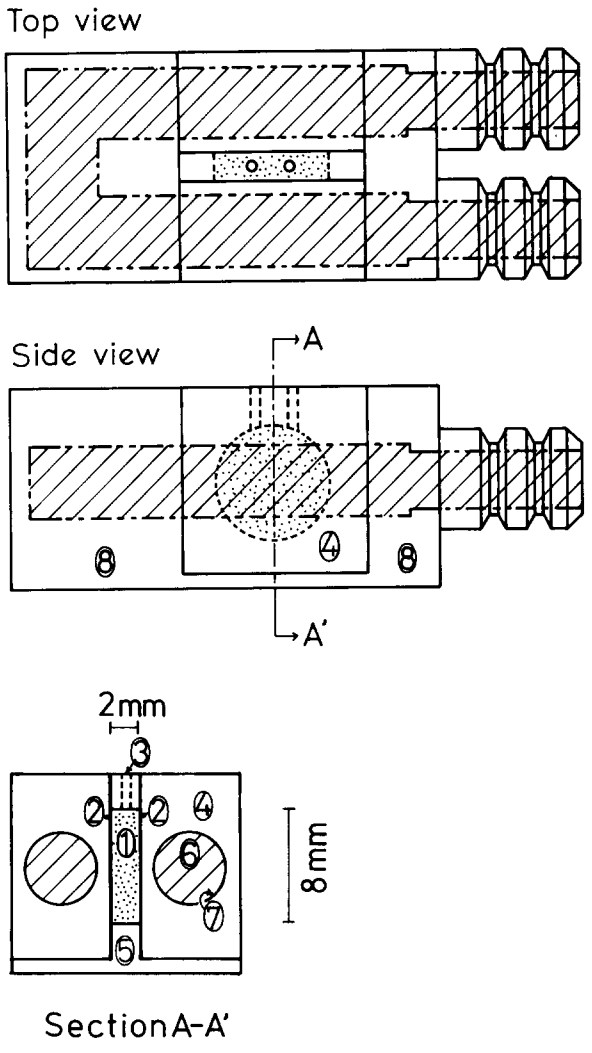

Fig. 1. Diagram of the thermostated permittivity cell composed of: (1) sample cavity (100 μl), (2) platinized Pt-disc electrodes, (3) sample inlet, (4) brass block, (5) lucite spacer, (6) conduit for circulating water, (7) epoxy resin coating, and (8) lucite block.

frequency points over the above-mentioned range was completed within 2 min. A parallel-plate capacitor type measuring cell (Fig. 1) accommodating a 0.1-ml sample volume was constructed for the dual purposes of fitting the cell to the analyzer's test terminals and better thermal regulation of the sample cavity. The cell constant (0.22 pF) determined by a standard method agreed well with that predicted from the cell geometry. Raw data from the analyzers were routinely corrected for the

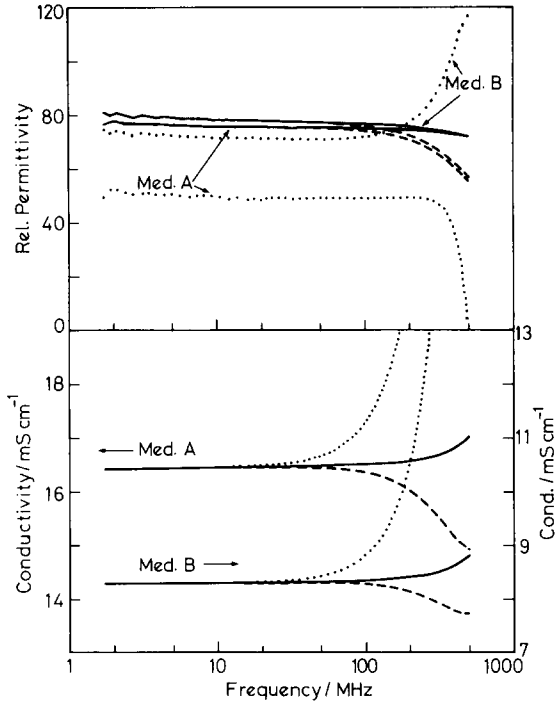

Fig. 2. Illustration of the correction methods as applied to data on medium A (virtually, 130 mM KCl) and medium B (65 mM KCl plus sucrose). Solid lines, corrected by the present method; broken lines, corrected by the method of Schwan [19]; dotted lines, uncorrected.

effects of series inductance and stray capacitance by assuming a distributed-parameters network model instead of the conventional lumped-parameters model (for details, see Appendix A). With the present method, correction was found to be more effective, especially for the frequency region above 50 MHz, than with the conventional one, as illustrated in Fig. 2.

Analysis

In the analysis of dielectric dispersion data, we employed a theory proposed by Hanai et al. [14] since the test suspensions at large were highly concentrated (volume fraction, 0.3–0.6). Fig. 3 shows the model on which the theory is based. Pertinent equations are briefly explained below.

The complex relative permittivity, ϵ^*, of a spherical suspension which is made up of uniform particles of radius R having equivalent homoge-

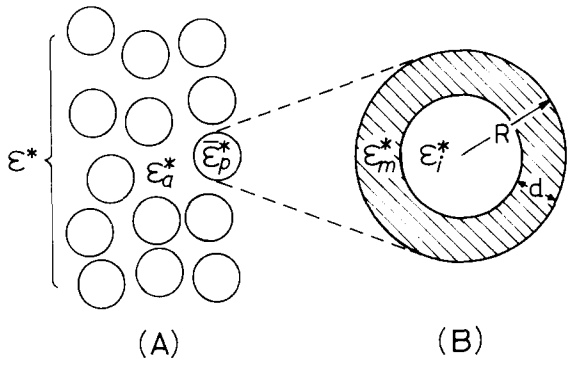

Fig. 3. Theoretical model for a concentrated suspension of membrane-covered particles. ϵ^* refers to the complex relative permittivity of a spherical suspension (A) in which the suspended phase (B) having an equivalent homogeneous permittivity $\bar{\epsilon}_p^*$ is dispersed in the continuous phase ϵ_a^*.

neous permittivity $\bar{\epsilon}_p^*$ and surrounded by a continuous medium of ϵ_a^* (Fig. 3A) is given by

$$\left(\frac{\epsilon^* - \bar{\epsilon}_p^*}{\epsilon_a^* - \bar{\epsilon}_p^*}\right)\left(\frac{\epsilon_a^*}{\epsilon^*}\right)^{1/3} = 1 - \phi \tag{1}$$

where ϕ is volume fraction. On the other hand, $\bar{\epsilon}_p^*$ is, in a sense, a temporary 'linkage' parameter allotted for the suspended phase of particles whose fine structure is detailed in Fig. 3B. $\bar{\epsilon}_p^*$ is expressed as

$$\bar{\epsilon}_p^* = \epsilon_m^* \frac{2(1-v)+(1+2v)E}{2+v+(1-v)E} \tag{2}$$

with $E = \epsilon_i^*/\epsilon_m^*$ and $v = (1 - d/R)^3$. Combination of Eqns. 1 and 2 gives a complete expression for the dielectric behavior of any suspensions, including relatively concentrated ones, of spherical shells such as represented by Fig. 3. The best-fit values of parameters for the membrane and the internal phase were determined using a curve-fitting method [14].

Results

Freshly prepared mitochondria (panel s, Fig. 4) assumed a characteristic conformation known as the 'condensed' form [15] when incubated at 4°C in the salt-free, sucrose medium. It is well established that such intact mitochondria in vitro tend to swell or contract under a variety of conditions [16]. In fact, our examination under the electron microscope revealed the swelling of mitochondria when incubated in a KCl-containing medium at an elevated temperature, say, 25°C. In view of these variable temperature and ionic effects on the mitochondrial structure, two temperatures (4 and 25°C) in combination with two ionic strengths (65 and 130 mM KCl) were chosen as the test conditions in the present study.

Fig. 4 (panels a–c) shows a typical morphology of the mitoplasts that were derived from intact mitochondria in a hyposmotic medium and fixed immediately after the dielectric measurements. As seen in panels a and b, the mitoplasts that were deprived of the outer membrane remained substantially shrunken at 4°C while, at 25°C, they became swollen with less dense cores. The stereologically averaged radii of the particles as shown in panels a and b were calculated to be 0.41 and 0.50 μm, respectively. No significant difference in the particle size was observed between the mitoplasts incubated in media A and B. The mitoplasts, once made swollen by incubation at 25°C for 1 h, never resumed the shrunken state even by a further 1-h incubation at 4°C, as shown in panel c. These contrasting features in morphology prompted us to examine the mitoplasts under the dielectric dispersion measurements described below.

Fig. 5 shows the dielectric behavior observed with the same specimens as represented by Fig. 4 (a–c). As clearly shown by dotted curves b in Fig. 5, the mitoplast suspension in an isotonic KCl solution at 25°C exhibited a marked frequency-dependent change in its relative permittivity and conductivity with a characteristic frequency of about 20 MHz, being in good agreement with the data of Pauly et al. [2] on a similar mitochondrial suspension. To further characterize this behavior, the same data were plotted in the complex permittivity and conductivity planes (dotted lines b in Fig. 6) or the Cole-Cole plots [17]. According to the routine of this kind of plotting we can readily obtain five important phenomenological parameters. These include κ_l (low-frequency limit of κ), ϵ_l (low-frequency limit of ϵ), ϵ_h (high-frequency limit of ϵ), f_c (characteristic frequency), and θ (degree of depression of center). By applying the values of

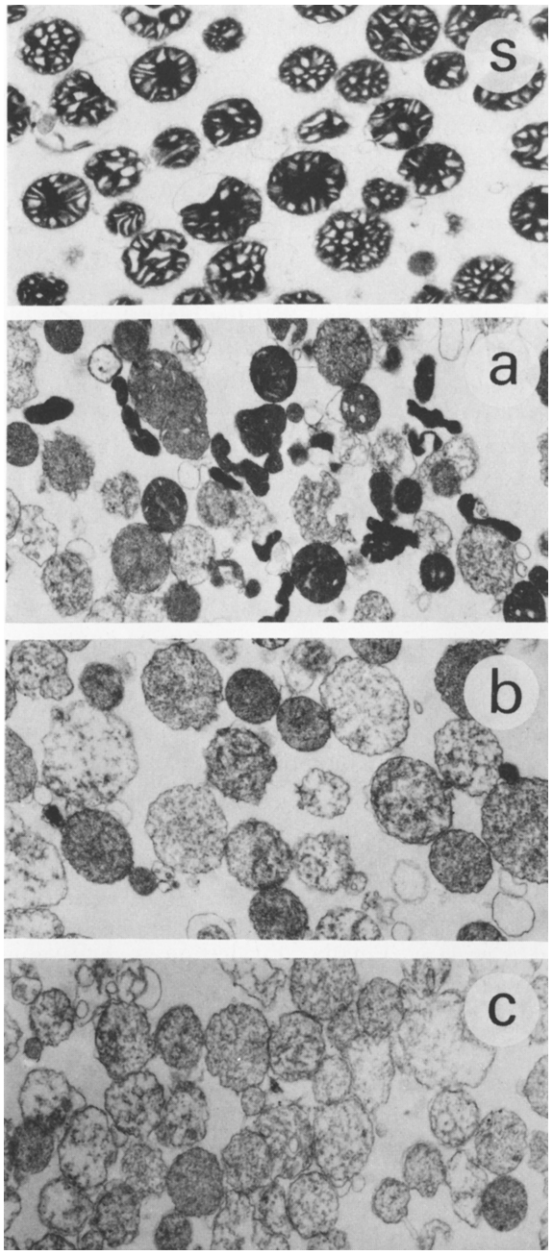

Fig. 4. Electron micrographs of intact mitochondria (s) suspended in the EDTA-free preparation medium at 4°C and swollen mitoplasts (a–c) incubated for 1 h, prior to fixation, in medium A at different temperatures: (a) 4°C, (b) 25°C, and (c) 4°C after 1-h preincubation at 25°C. Magnification, 10000×.

these parameters to the widely accepted Cole-Cole formula [17]:

$$\epsilon^* = \epsilon_h + \frac{\Delta\epsilon}{1+(jf/f_c)^{\beta}} + \frac{\kappa_l}{2\pi jf\epsilon_v} \qquad (3)$$

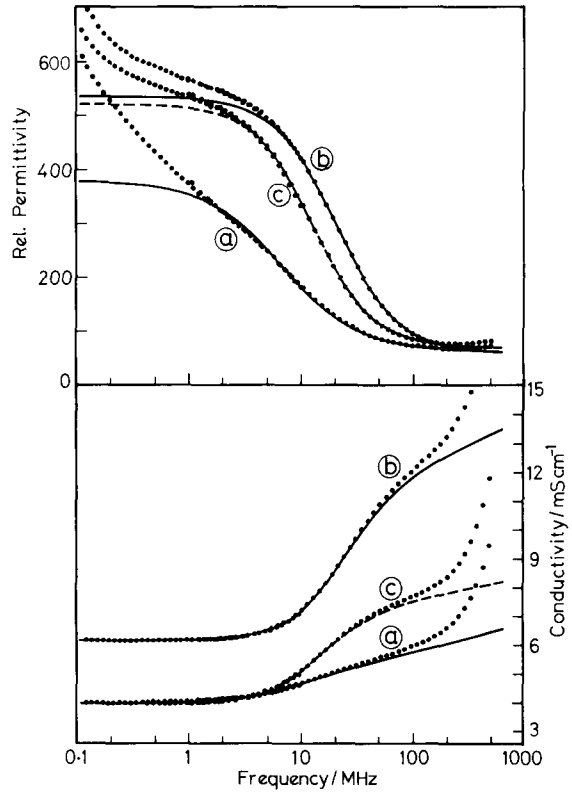

Fig. 5. Frequency dependence of ϵ and κ for mitoplasts suspended in medium A. Incubation conditions for the samples represented by curves a–c are the same as in legend to panels a–c in Fig. 4. "Temperature/volume concentration ϕ" of the specimens under dielectric measurements: (a) 4°C/0.444 (b) 25°C/0.487 and (c) 4°C/0.460. Solid and broken lines denote the best-fit theoretical curves predicted from Eqn. 3 with the following parameters: (a) $\epsilon_h = 59$, $\Delta\epsilon = 322$, $\kappa_l = 3.99$ mS/cm, $f_c = 6.8$ MHz, $\beta = 0.82$; (b) $\epsilon_h = 56$, $\Delta\epsilon = 480$, $\kappa_l = 6.14$ mS/cm, $f_c = 20.8$ MHz, $\beta = 0.91$; (c) $\epsilon_h = 67$, $\Delta\epsilon = 453$, $\kappa_l = 3.93$ mS/cm, $f_c = 12.9$ MHz, $\beta = 0.93$.

where $\Delta\epsilon = \epsilon_l - \epsilon_h$, $\beta = \theta°/90°$, $j = (-1)^{1/2}$ and $\epsilon_v = 8.854 \cdot 10^{-12}$ F/m, we can simulate the experiment by a numerical means. The result of one such simulation is illustrated by solid curves b in Figs. 5 and 6.

Fitting was satisfactory except for some deviations at very low (for ϵ) as well as very high (for κ) frequencies. The former deviation was largely due to the electrode polarization while the origin of the latter remains to be identified. Another point worthy of note is that, if we assume the formalism of Eqn. 3 to be the case, then the plots of complex

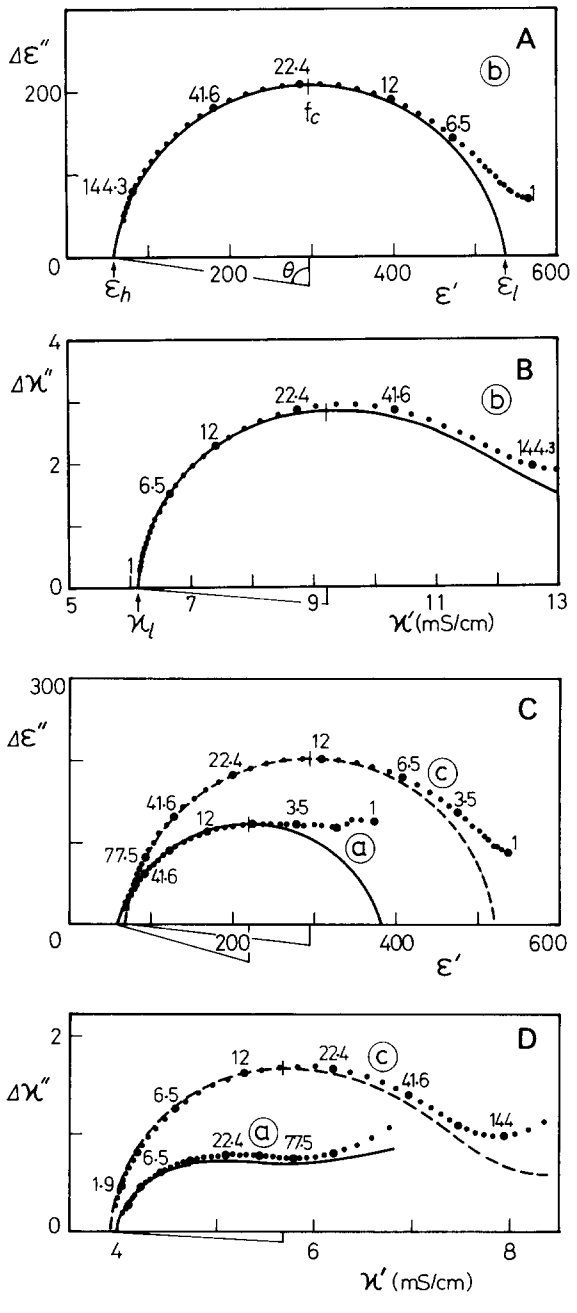

Fig. 6. Complex plane plots of data in Fig. 5. Solid or broken lines and marks a–c both correspond to those of Fig. 5. The number on each point refers to marker frequency in MHz; the vertical bar on top of the circular trace indicates characteristic frequency, f_c.

conductivity, viz., the relation between $\Delta\kappa''(= 2\pi f(\epsilon - \epsilon_h)\epsilon_v)$ and $\kappa'(=\kappa)$, in general do not conform to the 'circular arc' rule; it is only when $\beta = 1$ that the circular traces ensue in the plots of both ϵ^* and κ^*. In Figs. 5 and 6 are also documented the results of such simulation for the other two specimens corresponding to panels a and c (Fig. 4). The circular plots for the shrunken mitoplasts (curves a) were most depressed relative to the others, indicating that the highest degree of heterogeneity was involved in the electrical and/or morphological properties of this particular specimen.

In any case, with these parameters in hand, we can start analysis of the observed dielectric behavior on the basis of the shell model (Fig. 3). As an example, our procedure as applied to specimen b will be outlined below. First, a ϕ-value of 0.487 is determined from the relation [18]:

$$\phi = 1 - (\kappa_i/\kappa_a)^{2/3} \tag{4}$$

which is readily derived from the general equation (Eqns. 1 and 2 as combined) on the reasonable assumption that $\kappa_m \ll \kappa_a$; actually, we put $\kappa_m \leq \kappa_a \cdot 10^{-5}$. Next, with the ϕ value fixed, the values of ϵ_m and ϵ_i, respectively, and in this order, are searched for so that the calculated ϵ_l and ϵ_h fit to those observed. At this stage we have $\epsilon_m = 7.63$ and $\epsilon_i = 47.1$. Finally, by letting a half-value frequency $f_{1/2}$ (defined as the frequency at which $\epsilon = \epsilon_h + (\Delta\epsilon/2)$ fit the observed f_c (= 20.8 MHz), the interior conductivity κ_i is determined to be 9.33 mS/cm. The membrane capacity, C_m, of 0.97 μF/cm^2 is calculated from $C_m = \epsilon_m\epsilon_v/d$ with $d =$ 7.0 nm. The results obtained by such curve fittings are summarized in Table I.

A brief survey of Table I reveals that the parameters of shrunken mitoplasts (specimen a) differ considerably from those of swollen mitoplasts (specimens b and c) with the only exception for ϵ_m or its derived parameter C_m of approx. 1 μF/cm^2. In specimen a, the internal permittivity ($\epsilon_i \simeq 33$) and the conductivity ratio ($\kappa_i/\kappa_a \simeq 0.17$) were smaller than those for specimens b and c irrespective of the two different temperature and medium conditions employed. Between specimens b and c, ϵ_m (or C_m) and κ_i/κ_a were both substantially similar.

TABLE I

SUMMARY OF PASSIVE ELECTRICAL PARAMETERS FOR MITOPLASTS IN MEDIA A AND B AT THE TEMPERATURES OF 4 AND 25°C

Values are expressed as the mean ± S.E. of n separate determinations. Fixed parameters used for the analysis are given in the format, 'parameter: value ± S.E. (medium type, temperature in °C)': ϵ_a: 86.2 ± 0.3 (A, 4), 86.6 ± 0.2 (B, 4), 76.6 ± 0.7 (A, 25), 77.2 ± 0.8 (B, 25); κ_a in mS/cm: 9.43 ± 0.22 (A, 4), 4.62 ± 0.08 (B, 4), 15.95 ± 0.36 (A, 25), 8.16 ± 0.19 (B, 25). Medium A, 130 mM KCl in 10 mM Tris-HCl (pH 7.4); Medium B, 65 mM KCl in the same buffer supplemented with sucrose to make medium B isosmotic with medium A.

Medium	Temp. (°C)	n	ϵ_m	ϵ_i	κ_i (mS/cm)	C_m (μF/cm^2)	ϵ_i/ϵ_a	κ_i/κ_a
(a) A	4	3	7.4 ± 0.3	34 ± 3	1.81 ± 0.07	0.94 ± 0.04	0.39 ± 0.03	0.19 ± 0.01
B	4	3	7.1 ± 0.1	31 ± 1	0.67 ± 0.06	0.89 ± 0.02	0.36 ± 0.01	0.14 ± 0.01
(b) A	25	6	7.5 ± 0.3	48 ± 1	8.64 ± 0.31	0.95 ± 0.04	0.62 ± 0.01	0.54 ± 0.03
B	25	5	7.8 ± 0.3	49 ± 2	4.86 ± 0.16	0.99 ± 0.04	0.64 ± 0.03	0.60 ± 0.01
(c) A	4 [a]	3	8.0 ± 0.1	57 ± 3	5.77 ± 0.14	1.01 ± 0.01	0.66 ± 0.03	0.60 ± 0.01
B	4 [a]	3	8.1 ± 0.1	61 ± 3	3.00 ± 0.01	1.02 ± 0.02	0.70 ± 0.02	0.64 ± 0.01
Mean ± S.E.		23 or 17	7.6 ± 0.1			0.97 ± 0.02	0.65 ± 0.01 [b]	0.58 ± 0.01 [b]

[a] Preceded by 1-h incubation at 25°C.

[b] Calculated by omitting numbers on top two lines.

Discussion

Our experiments confirm Pauly, Packer and Schwan's pioneering, now classical, observations [2,3] that the swollen mitochondrial suspensions show a remarkable dielectric dispersion of the type termed 'β-dispersion' [19], the characteristic frequencies of which are claimed to fall in the range 1–100 MHz for the particles of about micrometer size. However, differences have arisen, between ours and theirs, in several points of the analysis and hence in the parameter values obtained. Comments are itemized below.

Measurements and corrections

As noted in the methods section, the impedance analyzer readings required proper corrections for artefacts caused by the series inductance and capacitance effects before the analysis of data was started. To this end we employed a distributed-parameters model instead of the conventional lumped-parameter approximation (Appendix A). As shown in Fig. 2, corrections for the inductance and stray capacitance effects that were inherent in the present type of cell assembly were so effective as to improve the reliability of the dispersion measurements, especially in the high-frequency region. However, there still remained a small and systematic increase in κ around 200 MHz or higher (Fig. 2). Such an increase in κ might not have been entirely due to artefact but rather due to a real phenomenon because available evidence [20] indicates that the dielectric dispersion of water may have begun to take place at these 'subgigahertz' frequencies.

Another improvement has been made in the measurement system in that the frequency scanning over four decades was feasible within 2 min. This was not only favorable to biological membrane samples susceptible to deterioration under prolonged measurements but was rather essential to monitoring time-dependent changes, if any, in their dielectric behavior [21]. All in all, the measurement itself has become much more reliable with the present system than with the manually operated bridge method.

The Cole-Cole plots

As well known, when a complex permittivity diagram (e.g., Fig. 6, A and C) traces a circular arc, its empirical formalism may be given by Eqn. 3. On the other hand, Eqn. 3 does not necessarily guarantee a similar 'circular' curve to the plots of corresponding complex conductivities as exem-

plified in Fig. 6 (B, D). This stems from the very nature of Eqn. 3 or the circular arc rule. The same subject has been pointed out also by Stoy et al. [22]. In fact, our analysis of the behavior of complex conductivity κ^* defined as

$$\kappa^* = \kappa' + j\kappa'' = j\omega\epsilon_v\epsilon^* \tag{5}$$

with $\omega = 2\pi f$, revealed that if $\beta < 1$ in Eqn. 3 then neither of the real and the imaginary parts of κ^* do converge as frequency tends to infinity (see Appendix B). Thus it is only when $\beta = 1$ that a finite value is also shared by κ in the high-frequency limit.

In the light of the argument above, the analytic procedure of Pauly et al. [2] appears to be somewhat misleading in point of their reliance upon κ_h (high-frequency 'limiting' value of κ) and $f_{c\kappa}$ ('center' frequency read from the κ^* plots). Suffice it to say that when $\beta < 1$ these two parameters are more or less of an arbitrary nature so that their physical meanings lose ground as far as the combination of Eqn. 3 and 5 is strictly maintained. For the reason above our analysis presented here used exclusively the parameter values obtainable from the Cole-Cole plots for ϵ^*.

Comparison of the two theories as judged from curve fittings

In the analysis of data by the curve fitting procedure we employed Hanai-Asami-Koizumi's theory (Eqns. 1 and 2) by virtue of its claimed applicability to the concentrated suspension of spherical particles [6,23]. Indeed, as clearly shown in Fig. 7, fitting between theory and experiment was more than satisfactory at least over the frequency range spanning about two decades across the center frequency f_c, though outside this range with some systematic deviations of the experimental points. However, no blame should be put upon the theory since the deviation at lower frequencies was essentially due to electrode polarization. As for a steep rise in κ in the subgigahertz region, the following two mechanisms must have been involved. One is contribution from the dispersion of water [20]; the other which is also highly likely may be structural and/or molecular relaxation occurring inside the mitoplasts. At least, any membranous 'substructure' like cristae was not responsible for this issue because the swollen mitoplasts lacked such an internal membrane system (Fig. 4).

In Fig. 7 are also included a pair of best-fit curves (broken lines) calculated from the general equation of Pauly-Schwan's theory [4,5] of the form:

$$\frac{\epsilon_a^*/\epsilon^* - 1}{2\epsilon_a^*/\epsilon^* + 1} = \frac{(2+E)(F-1)+(1-E)(F+2)v}{(2+E)(2F+1)+2(1-E)(F-1)v}\phi \tag{6}$$

where $E = \epsilon_i^*/\epsilon_m^*$, $F = \epsilon_a^*/\epsilon_m^*$ and $v = (1 - d/R)^3$. Note that Eqn. 6 has been derived by assuming a dilute suspension in which interparticulate interaction is negligible, or mathematically $\phi \ll 1$. Otherwise, the validity of Eqn. 6 should be questionable. As seen in Fig. 7, difference between the two theories in the fittedness to experiment is apparent in spite of the same values of parameters (κ_l, ϵ_l, ϵ_h, and f_c) being used. Table II compares the values of the phase parameters analyzed according to the theories of Hanai, Asami and Koizumi and of Pauly and Schwan as applied to one typical experiment. In this example where $\phi \simeq 0.6$, the difference was remarkable in ϵ_m (or C_m), moderate in ϕ and almost nil in the internal phase parameters, ϵ_i and κ_i.

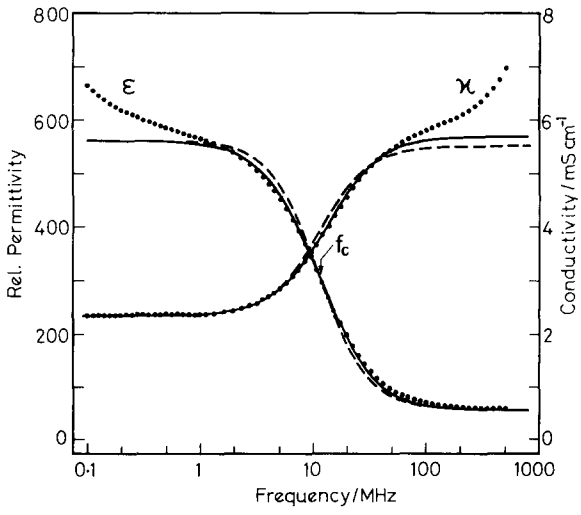

Fig. 7. Curve fittings by Pauly-Schwan's (------) and Hanai-Asami-Koizumi's (————) theories of data (·····) on mitoplasts suspended in medium B at 25°C. Parameters employed, as in Table II.

TABLE II

COMPARISON OF PARAMETERS DEDUCED FROM HANAI-ASAMI-KOIZUMI'S THEORY ('H-A-K') AND PAULY-SCHWAN'S THEORY ('P-S')

Calculations employ data [a] in Fig. 7 and the following fixed parameters: $\epsilon_a = 75.5$, $\kappa_a = 8.67$ mS/cm, $\kappa_m = \kappa_a \cdot 10^{-5}$, $R = 0.498$ μm and $d = 7.0$ nm.

Theory	ϵ_m	ϵ_i	κ_i (mS/cm)	ϕ	C_m (μF/cm^2)
'H-A-K'	7.04	49.2	4.86	0.583	0.89
'P-S'	9.31	50.6	4.78	0.644	1.18
% Difference [b]	32.2	2.8	−1.6	10.4	32.2

[a] $\epsilon_l = 562$, $\epsilon_h = 56$, $\kappa_l = 2.34$ mS/cm and $f_c = 11.3$ MHz.
[b] Expressed as deviations of 'P-S' values from 'H-A-K' values.

Implication of the phase parameters

As noted in Results, specimen a was apparently heterogeneous in its morphology, being a mixture of varying degrees of both shrunken and swollen mitoplasts. This situation was also reflected in its dispersion behavior (Figs. 5 and 6) and hence in the assigned values listed in Table I. For this reason we refrain from making any serious comments on specimen a.

It is reasonable that the parameters associated with the outermost phase (i.e., the limiting membrane) were more readily determined than those of the interior phase. Our analysis assuming the membrane to be 7.0 nm thick gave an ϵ_m-value of 7.5–8.1 or alternatively a membrane capacitance (C_m) of 0.96–1.02 μF/cm^2 which is very close to the accepted value of C_m for the plasma membranes. In addition, the mitoplasts when swollen were virtually free from wrinkles or infoldings on their surface (Fig. 4) and the C_m value of 1 μF/cm^2 was a plausible estimate accordingly. This finding in turn indicates that the mitochondrial inner membranes (i.e., the mitoplast envelope) have much in common with the cell membrane at least in the basic molecular organization as reflected on C_m. The C_m values of approx. 0.5 μF/cm^2 reported by Pauly et al. [2] on a similar specimen was probably an underestimate.

Equivalent homogeneous conductivity for the mitoplast interior (κ_i) turned out to be about 60% of the medium conductivity (κ_a) almost independent of the incubation conditions employed. In this regard we agree with Pauly et al. [2]. Such a lowering of κ_i in spite of the near-complete equilibration with the test media implies that the effective concentration (or activity) of the total ions responsible for κ_i was reduced by partial sequestration within the matrical space and, in addition, that the mobility of free small ions was retarded by the viscosity effect due to the intramatrical protein in high concentration. It may be relevant to note that we determined protein for every specimen tested and then calculated the specific volume of mitoplasts (v) given by the ratio, a volume fraction (ϕ) divided by the corresponding protein concentration. The mean values of v for specimens a, b and c, all in medium A, were determined to be 3.7, 7.4 and 8.4 μl/mg protein (on the albumin basis), respectively. Taking the reciprocal of v we can make an estimate of the order 0.1 g/ml of the apparent protein content in the mitoplasts. The reduction of ϵ_i relative to ϵ_a (Table I) may also be attributable to the protein effect.

Appendix A

Here we present a brief account of the correction method based on a distributed-parameters network model. Fig. 8 shows two pertinent models, of which network (a) is our immediate concern and can be regarded as a two-ports Lecher line;

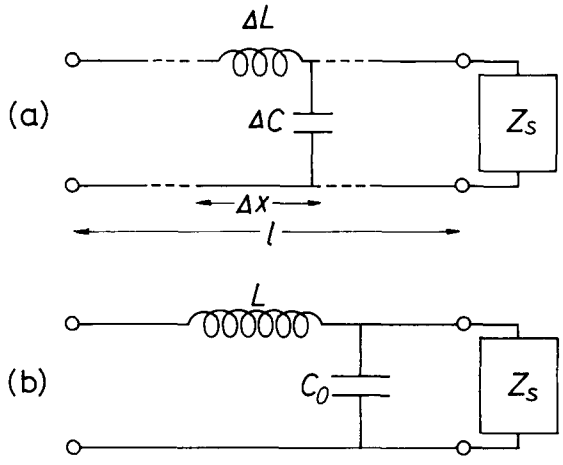

Fig. 8. Equivalent-circuit models used for the correction of impedance analyzer readings: (a) distributed-parameters network, (b) lumped-parameter network.

network (b) is the conventional lumped-parameter model.

Consider a uniform, loss-free Lecher line of length l such as depicted in Fig. 8a. Textbooks on circuit analysis teach that its characteristic impedance, Z_0', and propagation constant, γ', are given by

$$Z_0' = \sqrt{L'/C'} \tag{A1}$$

$$\gamma' = \sqrt{L'C'} \tag{A2}$$

where L' and C' are, respectively, inductance and capacitance per unit length of the line. If the two-ported line is loaded with an impedance Z_s, then the imput impedance, Z_i, of the resulting composite one-port line is expressed as

$$Z_i = Z_0' \frac{Z_0' \sinh \gamma' l + Z_s \cosh \gamma' l}{Z_0' \cosh \gamma' l + Z_s \sinh \gamma' l} \tag{A3}$$

On the other hand, one may write down

$$1/Z_s = G_s + j\omega C_s,\ 1/Z_i = G_i + j\omega C_i \tag{A4}$$

where G and C are equivalent parallel conductances and capacitances with subscripts, s and i, referring to the sample and input impedances, respectively, and ω is angular frequency. Now, combining Eqns. A1–A4 and solving for G_s and C_s we have

$$G_s = \frac{G_i}{(\cos\omega\gamma + \omega C_i Z_0 \sin\omega\gamma)^2 + (G_i Z_0 \sin\omega\gamma)^2} \tag{A5}$$

$$C_s = \frac{1}{2\omega} \cdot \frac{(Z_0 G_i^2 + \omega^2 Z_0 C_i^2 - 1/Z_0) \sin 2\omega\gamma + 2\omega C_i \cos 2\omega\gamma}{(\cos\omega\gamma + \omega C_i Z_0 \sin\omega\gamma)^2 + (G_i Z_0 \sin\omega\gamma)^2} \tag{A6}$$

where $\gamma = (LC_0)^{1/2}$ and $Z_0 = (L/C_0)^{1/2}$ with $L = L'l$ and $C_0 = C'l$. Quite similarly, we have

$$C_i = \frac{-1}{2\omega} \cdot \frac{(Z_0 G_s^2 + \omega^2 Z_0 C_s^2 - 1/Z_0) \sin 2\omega\gamma - 2\omega C_s \cos 2\omega\gamma}{(\cos\omega\gamma - \omega C_s Z_0 \sin\omega\gamma)^2 + (G_s Z_0 \sin\omega\gamma)^2} \tag{A7}$$

In the low-frequency limit ($\omega \to 0$) we obtain, from Eqns. A5 and A7, the following simple relations:

$$G_i = G_s \tag{A8}$$

$$C_i = C_s + C_0 - LG_s^2 \tag{A9}$$

The last two equations as they stand apply to the lumped-parameter model (Fig. 8b) when $\omega \to 0$. In fact, the method of Schwan [19] is based on Eqns. A8 and A9. One may readily obtain the values of $C_s + C_0$ and L by plotting C_i against G_i^2 measured with a series of aqueous KCl solutions in the low-frequency range. The stray capacitance C_0 and the cell constant C_1 are determined from measurements with the empty cell or the cell filled with deionized water since, in either case, Eqn. A9 reduces to

$$C_i = C_s + C_0 \tag{A10}$$

at low enough frequencies. Here, $C_s = C_1$ for air and $C_s = C_1 \times \epsilon_{H_2O}$ for water. In the present study we employed a correction method that was based on Eqns. A5 and A6 and coupled with the determined values of L and C_0.

Appendix B

The complex forms of ϵ and κ, interrelated through text Eqn. 5, may be written as

$$\epsilon^* = (\Delta\epsilon' + \epsilon_h) - j(\Delta\epsilon'' + \kappa_1/\omega\epsilon_v) \tag{B1}$$

$$\kappa^* = (\Delta\kappa' + \kappa_1) + j(\Delta\kappa'' + \omega\epsilon_v\epsilon_h) \tag{B2}$$

so that

$$\Delta\kappa' = \omega\epsilon_v\Delta\epsilon'' \tag{B3}$$

$$\Delta\kappa'' = \omega\epsilon_v\Delta\epsilon' \tag{B4}$$

On the other hand, comparison of Eqn. B1 and text Eqn. 3 leads to

$$\Delta\epsilon' - j\Delta\epsilon'' = \frac{\Delta\epsilon}{1 + (j\omega\tau)^\beta} \tag{B5}$$

where $\tau = 1/2\pi f_c$. By separation of the real and imaginary parts of Eqn. B5 followed by combination with Eqns. B3 and B4, we have the following

version of $\Delta\kappa'$ and $\Delta\kappa''$, both as a function of ω:

$$\Delta\kappa' = \frac{A\omega^{\beta+1}}{1 + B\omega^{\beta} + C\omega^{2\beta}} \tag{B6}$$

$$\Delta\kappa'' = \frac{A'\omega^{\beta+1} + B'\omega}{1 + B\omega^{\beta} + C\omega^{2\beta}} \tag{B7}$$

where A, A', B, B' and C are all finite and independent of ω. Therefore, if $\beta < 1$, Eqns. B6 and B7 should turn to infinity as $\omega \to \infty$.

Acknowledgments

We wish to thank Mrs. T. Ichinowatari and Mr. K. Yagiu for their skillful technical assistance. This work was supported in part by grants 548089, 56770052, and 56870020 from The Ministry of Education, Science and Culture, Japan.

References

1 Lehninger, A.L. (1982) Principles of Biochemistry, Chapters 2 and 17, Worth Publishers, New York
2 Pauly, H., Packer, L. and Schwan, H.P. (1960) J. Biophys. Biochem. Cytol. 7, 589–601
3 Pauly, H. and Packer, L. (1960) J. Biophys. Biochem. Cytol. 7, 603–612
4 Pauly, H. and Schwan, H.P. (1959) Z. Naturforsch. 14b, 125–131
5 Hanai, T., Koizumi, N. and Irimajiri, A. (1975) Biophys. Struct. Mech. 1, 285–294
6 Zhang, H.Z., Sekine, K., Hanai, T. and Koizumi, N. (1983) Colloid Polymer Sci. 261, 381–389
7 Asami, K. and Irimajiri, A. (1984) Biochim. Biophys. Acta 778, 570–578
8 Hogeboom, G.H. (1955) Methods Enzymol. 1, 16–19
9 Utsumi, K. (1963) Acta Med. Okayama 17, 259–271
10 Hartree, E.F. (1972) Anal. Biochem. 48, 422–427
11 Spurr, A.R. (1969) J. Ultrastruct. Res. 26, 31–43
12 Weibel, E.R. and Bolender, R.P. (1973) in Principles and Techniques of Electron Microscopy: Biological Application (Hayat, M.A., ed.), Vol. 3, pp. 237–296, Van Nostrand Reinhold, New York
13 Weibel, E.R. and Paumgartner, D. (1978) J. Cell Biol. 77, 584–597
14 Hanai, T., Asami, K. and Koizumi, N. (1979) Bull. Inst. Chem. Res. Kyoto Univ. 57, 297–305
15 Hackenbrock, C.R. (1966) J. Cell Biol. 30, 269–297
16 Lehninger, A.L. (1959) J. Biol. Chem. 234, 2187–2195
17 Cole, K.S. and Cole, R.H. (1941) J. Chem. Phys. 9, 341–351
18 Irimajiri, A., Hanai, T. and Inouye, A. (1975) Experientia 31, 1373–1374
19 Schwan, H.P. (1963) in Physical Techniques in Biological Research (Nastuk, W.L., ed.), Vol. 6B, pp. 323–407, Academic Press, New York
20 Schwan, H.P., Sheppard, R.J. and Grant, E.H. (1976) J. Chem. Phys. 64, 2257–2258
21 Asami, K. and Irimajiri, A. (1984) Biochim. Biophys. Acta 769, 370–376
22 Stoy, R.D., Foster, K.R. and Schwan, H.P. (1982) Phys. Med. Biol. 27, 501–513.
23 Sekine, K., Hanai, T. and Koizumi, N. (1983) Bull. Inst. Chem. Res., Kyoto Univ. 61, 299–313.